

# Low Velocity Impact Behaviour of Aramid and UHMWPE Composites

Uludag University Vocational School  
of Technical Sciences,  
Görükle-Bursa Turkey  
E-mail: mkarahan@uludag.edu.tr

\*Department of Fiber and Polymer Engineering,  
Faculty of Natural Sciences,  
Architecture and Engineering  
Bursa Technical University,  
Bursa TR-16059 Turkey

## Abstract

The most popular method to produce composites for ballistic applications is to use aramid and ultra high molecular weight polyethylene (UHMWPE) fibers as reinforcement materials in different matrices. The composite materials used in this type of application, especially those used as armoring materials for explosions, are subjected to a very high level of energy. In this study, the effect of the reinforcement material type and cross-ply condition of reinforcement were examined using high-level impact tests. The impact tests were performed at low speed but high energy, and thus the behaviour of the composite materials that were exposed to high-level impact energy could be examined. According to the results, the UD aramid composite produced the best results with respect to high-level impact tests. In addition, mass optimisation could be achieved without the loss of the high-level impact energy by preparing a hybrid composite with UD UHMWPE and UD aramid fibers.

**Key words:** aramid fibers, UHMWPE fibers, hybrid composites, low velocity impact.

## Introduction

Fibre-reinforced laminated composites have been used extensively in load-bearing structures generally due to their light-weightness, high strength-to-weight and stiffness-to-weight ratios, good corrosion resistance and reduction of parts count.

The low velocity impact behaviour of composite laminates has been studied extensively in recent decades. As described in two review papers [1, 2], experimental results reported in the literature have mainly focused on impact-induced damage mechanisms, such as matrix cracking, delamination and fibre breakage at different impact stages. However, most of the analytical methods have focused on the elastic impact on laminates with perfect boundaries. In addition to direct investigation of the laminate damage using the naked eye, such as for glass/epoxy laminates that are partially light transparent [3 - 5], C-scans or X-rays have generally been employed in damage assessment [6, 7].

Various solutions for improving damage tolerance have been developed, for example, by modifying the composite system with a toughened matrix [8], interleav-

ing [9], stitching [10] or z-pinning [11], which have resulted in varying degrees of success. Nevertheless the benefits of a cost-effective solution materialise only if the allowable strain is further increased. This requirement undoubtedly demands a thorough understanding of the impact response, damage mechanism and damage assessment of the composite structure.

The effect of damage is examined using one of two related approaches, namely impact damage resistance or damage tolerance. Impact damage resistance focuses extensively on the identification of the onset of the dominant damage mechanism (for example, delamination) from impact response curves in terms of the impact energy or energy absorbed.

The apparatus that typically determines the impact energy is a drop weight tower. Due to the limitation of the tower height, almost all the impact events are conducted using a heavy impactor at a low velocity of less than 10 m/s. The impact force is typically recorded using a force transducer embedded in the impactor. The corresponding histories of energy, velocity and displacement are then derived once the onset of contact between

the impactor and target, as determined by Cantwell and Morton [12].

However, higher speed and energy level impact results published in the literature have been far fewer than those for lower speed impact. One reason has been the need for a gas gun to provide the initial kinetic energy of the impactor. In this category, the impact has generally been conducted using a lighter impactor, generally called a projectile, at a much higher initial velocity. Furthermore because it is difficult to mount a sensor on a flying projectile [13, 14], the data recorded during such an impact event has usually only been the initial and final states of the projectile and the target. The history of the impact, even if a high-speed camera was employed, was difficult to record.

Recently ultrahigh molecular weight polyethylene (UHMWPE) fibre-reinforced composites have been widely used in applications due to their outstanding properties. The high impact resistance of these composites is one of the many advantages of UHMWPE fibre-reinforced composites. However, UHMWPE fibres exhibit low thermal resistance and poor adhesion to polymer matrices due to

**Table 1.** Parameters of reinforcements used in the study (specifications of the manufacturers).

Reinforcement definition	Aramid woven fabric-CT 736	Aramid Bi-Axial non-crimp fabric-XA450	Aramid woven fabric-Artec	Aramid UD sheet-GS3000	UHMWPE UD sheet-Dyneema H62
Reinforcement code	R1	R2	R3	R4	R5
Weave	Plain woven	Bi-axial non-crimp fabric	Plain woven	UD	UD
Warp/fill (or 0 - 90 °) yarns	Twaron 2000/ Twaron 2000	Twaron 2000/ Twaron 2000	Artec/Artec	Kevlar 49/Kevlar 49	Dyneema SK62/ Dyneema SK62
Linear density warp/fill, tex	336/336	336/336	58/58	126/126	176/176
Ends/picks counts, yarns/cm	12.7/12.7		11.6/11.6	-	-
Crimp warp/fill, %	0.8/0.8	Non-crimp	0.2/0.2	Non-crimp	Non-crimp
Areal density, g/m <sup>2</sup>	410	465	135	510	263
Reinforcement thickness, mm	0.6	0.40	0.23	0.50	0.25
Manufacturer	Teijin Aramid	Sartex	Pro-System	FMS Inc.	FMS Inc.

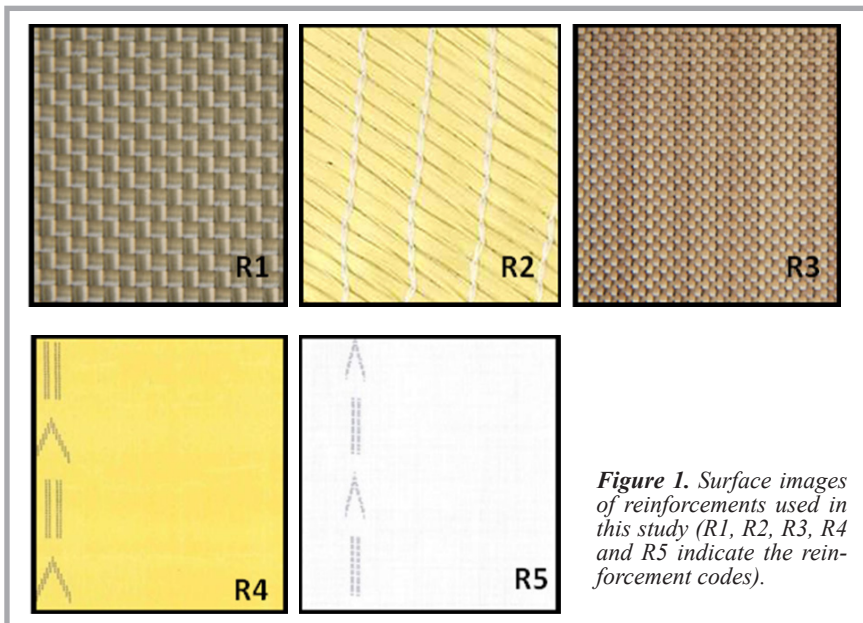


Figure 1. Surface images of reinforcements used in this study (R1, R2, R3, R4 and R5 indicate the reinforcement codes).

Table 2. Parameters of aramid and UHMWPE fibres used in the study (specifications of the manufacturers).

Parameters	Twaron 2000® (Aramid)	Artec® (Russian Aramid)	Kevlar 49® (Aramid)	Dyneema SK62® (UHMWPE)
Young modulus, GPa	85	103	112	113
Tenacity at break, cN/tex	235	181	208	338
Ultimate elongation, %	3.5	2.8	2.4	3.6
Density, g/cm <sup>3</sup>	1.44	1.44	1.44	0.97

chemical inertness and have limitations for structural applications. Aramid-fibre-reinforced composites are another type of composite that exhibit great performance, especially in terms of impact resistance [15 - 18]. Therefore aramid fibres can be hybridised into UHMWPE-

fibre-reinforced composites as a secondary reinforcing fibre to compensate for the disadvantages of UHMWPE mentioned above because of their good thermal resistance. The impact properties of hybrid composites are affected by many factors. For aramid fibre/UHMWPE fibre

hybrid composites, the hybrid type and ratio are two important factors.

The most popular method to produce composites for ballistic application is to use aramid and UHMWPE fibres as reinforcement materials in different matrices. The composite materials used in this type of application, especially those applied as armouring materials for explosions, are subjected to very high levels of energy. Because of that high energy level, impact tests provide more acceptable results because this type of composite material absorbs a high level of energy. The impact tester should have the capability of applying high-level energy onto the composite via a high level of speed of the striker.

In this study, the effect of the reinforcement material type, cross-ply condition of the reinforcement and the layer amount were examined using high-level energy impact tests, performed using low speed but with a high energy level; thus the behaviour of the composite materials that were exposed to this high impact energy could be examined.

## Experimental

Five different fibrous materials and three different hybrid structures were used as reinforcement in a low-density polyethylene (LDPE) matrix. Nolax A21.2007 LDPE adhesive film (density 0.94 g/cm<sup>3</sup>, melting temperature 80 - 90 °C and melt flow rate of 6 - 9 g/10 min) was used as a matrix system. The properties of the

Table 3. Properties of the composite plates.

Sample code	Reinforcement type	Reinforcement Ply number	Stacking direction	Resin	Plate thicknesses, mm	Sample weight, g/m <sup>2</sup>	Fibre volume fraction, %
A	R1	12	0°/90°	LDPE	5.05 ± 0.38	5050	54.6
B	R2	11	45°/-45°		4.96 ± 0.41	5190	52.5
C	R3	38	0°/90°		5.12 ± 0.26	5090	58.2
D	R4	13	0°/90°		4.99 ± 0.55	6680	68.2
E	R5	22	0°/90°		5.02 ± 0.48	5940	61.5
F	R1 + R2 (Hybrid)	6 + 6	0°/90°/45°/-45°		5.15 ± 0.58	5300	26.5 + 24.9
G	R1 + R3 (Hybrid)	6 + 19	0°/90°		4.93 ± 0.37	5025	25.4 + 27.8
H	R4 + R5 (Hybrid)	11 + 7	0°/90°		5.01 ± 0.50	6510	32.5 + 30.6

Table 4. Impact test results of samples at 1680 J energy level.

Samples	Peak load, N	Max. displacement, mm	Energy absorbed, J	Elastic recovery, J	Energy absorbed, %	Bending stiffness, N/mm
A	45944 ± 4447	52.36 ± 3.4	1469 ± 66.8	211	91.8	866 ± 32
B	31894 ± 1740	60.5 ± 5.5	1222 ± 210	458	76.3	701 ± 28
C	56374 ± 3181	41.3 ± 7.2	1388 ± 42	292	86.8	2350 ± 19
D	65285 ± 1420	32 ± 1.3	1467 ± 58	213	91.7	2710 ± 17
E	39039 ± 2283	51.13 ± 0.56	1406 ± 33	274	87.9	1157 ± 9
F	40399 ± 1051	56.31 ± 3.9	1293 ± 147	387	80.9	1627 ± 12
G	49354 ± 3381	48.03 ± 2.57	1466 ± 52	214	91.6	1543 ± 18
H	43308 ± 586	46.95 ± 1.23	1431 ± 43.5	249	89.5	2089 ± 21

reinforcement materials are provided in **Table 1**. Surface images of the reinforcements used in this study are presented in **Figure 1**. All the samples were produced in an autoclave. The temperature of the process was 110 °C, and the pressure of the vacuum 1.48 MPa. Basically the autoclave consolidation of composites is very simple: The laminate is vacuum bagged, evacuated inside to remove entrapped air, and then heated in order to melt the matrix material. As mentioned above, the process is relatively slow (320 minutes in total), but it is very suitable for material quality and the full wetting of fibres is guaranteed. In the first 20 minutes, after air is entrapped, the pressure and temperature are increased together to 0.8 MPa and 40 °C, respectively. In the next 100 minutes the pressure and temperature are raised gradually to 1.48 MPa and 110 °C, respectively. After standing for 100 minutes at this temperature and pressure, they are gradually decreased to the initial level in the next 100 minutes.

LDPE film becomes viscose liquid at 110 °C, result from the melting crystalline phase of the morphology. The amorphous phase of LDPE also melts under this temperature at a glass transition temperature of about -100 °C [19, 20]. This warm liquid easily wets the textile reinforcement materials under vacuum conditions.

The fibre properties are presented in **Table 2**. The fabrics used in the production of the composite materials were cut into 40 × 40 cm<sup>2</sup> pieces. **Table 3** lists the main production parameters of the composite samples such as the ply arrangements, number of fabric plies, and thickness of composite plates. The thicknesses of the finished samples were measured using a caliper. The thicknesses of all the composite sheets were approximately the same. The hybrid structures were manufactured with one surface composed of one reinforcement material and the other of the other reinforcement material.

The fibre volume fraction ( $V_f$ ) values presented in **Table 3** were obtained based on the fabric weight and plate thickness as follows:

$$V_f = n \cdot m / (\rho \cdot h) \quad (1)$$

where,  $n$  is the number of fabric plies,  $m$  the fabric areal weight,  $\rho$  the fibre density and  $h$  the plate thickness. The fibre volume fractions are calculated in both directions separately in the case of different warp and fill yarn densities. In **Table 3**,  $V_f$  values of hybrid samples (samples F,

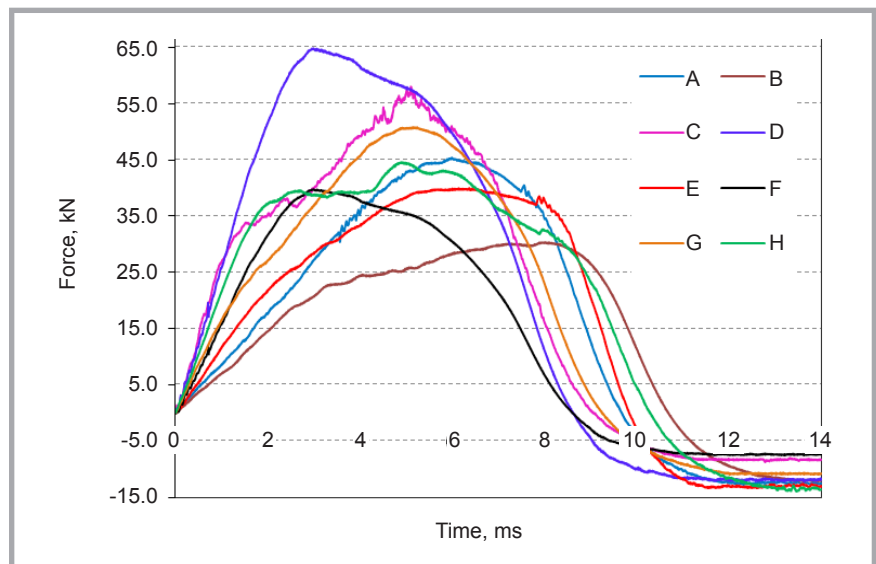


**Figure 2.** Typical impact load–time curves and comparisons of all samples (A, B, C, D, E, F, G and H indicate the sample codes - see **Table 3**).

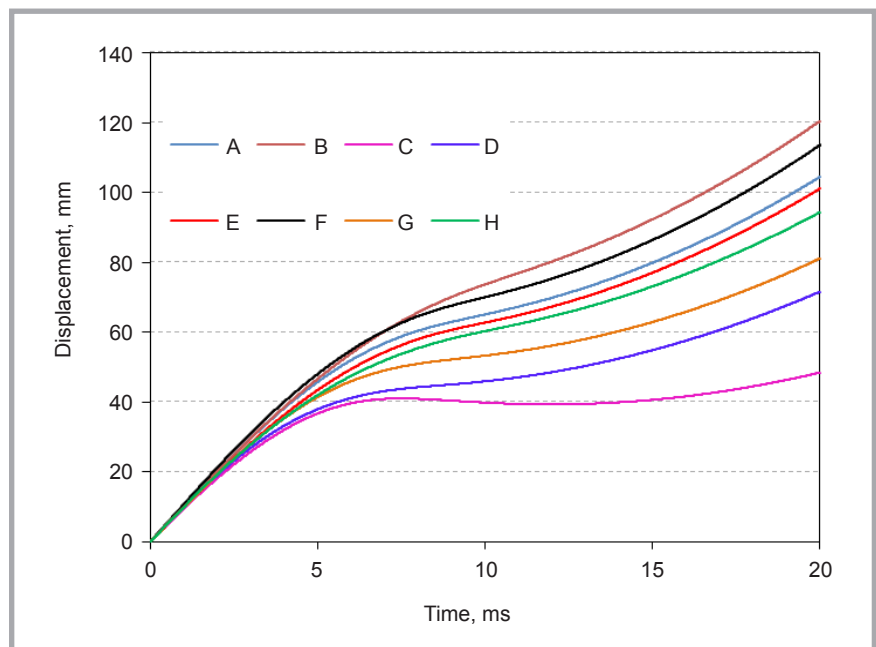


**Figure 3.** Typical impact displacement–time curves and comparisons of all samples (A, B, C, D, E, F, G and H indicate the sample codes).

G and H) were calculated for each reinforcement separately. Impact tests were performed on square section samples using an Instron CEAST Model 9350 tester according to the ASTM D3760 standard, and an impactor stroke was made at the centre of the samples using a circular support. The test mode was puncture, 90 kN, type 1, and a Ø 20 mm hemispheric geometry striker was used. The impact velocity, falling height, total impact energy applied, total falling mass, specimen support diameter and specimen clamping force were 10.5 m/s, 5621.2 mm, 1680 J, 30.5 kg, 70 mm and 18 kN, respectively. At least four tests were conducted for

each sample, and data on the load, energy, speed and deflection were recorded as a function of time.

## Results and discussion

### Low-velocity impact response and damage evaluation of samples

The present work aims to improve understanding of the behaviour of 100% aramid, 100% UHMWPE, aramid/aramid and aramid/UHMWPE hybrid composites and their modes of damage and failure behaviour under high energy levels, which is vital for the selection of appro-

appropriate materials for armouring applications. Low-velocity impact test results of all the composite samples are presented in **Table 4**, and force-time curves of all samples are given in **Figure 2**. Force-time curves for the hybrid composites are also presented in **Figure 2**, with those of the composites, from the hybrid structure they were produced, called 100% aramid or 100% UHMWPE composites for comparison.

The curve properties of all the samples were nearly the same after the peak point of the force, with force decreasing suddenly after the peak point. The slopes of the curves of all the samples in the elastic region were different, occurring due to the rigidity of the composites. The elastic region slope values are listed in **Table 4**, samples C and D being the most rigid. The displacement values also support this conclusion. The displacement-time curves are presented in **Figure 3**. More displacement implied higher deformation on the back surface of the composite. This conclusion could be verified by inspection of the deformation character of all the samples in **Figure 4**. Minimum deformation occurred for samples C and D, which also exhibited the highest rigidity. The top surface, bottom surface and cross-section of all the samples are shown in **Figure 4.a & 4.b**.

In terms of maximum force, the samples were ranked in the following order: C, D, G, A, F, E, H and B. Samples F and G were hybrid versions of samples B and C with sample A, respectively. These samples also produced good results. The maximum forces of all samples are provided in **Figure 5.a**.

The maximum force is related to the beginning of deformation of the samples. Before the maximum force, no deformation occurs in the material; however, after the point of maximum force, the materials undergo deformation. Deformation occurs with time until the point at which the material is completely broken down. In addition, continued deformation requires energy because energy absorption continues after the maximum force point. The time required to reach the maximum force is related to the rigidity of the material. For materials with greater rigidity, less time and less displacement were required to reach the maximum force and vice versa. This conclusion was also demonstrated by Aslan et al. [21] The displacement amount of the samples is a good indicator of the material rigidity.

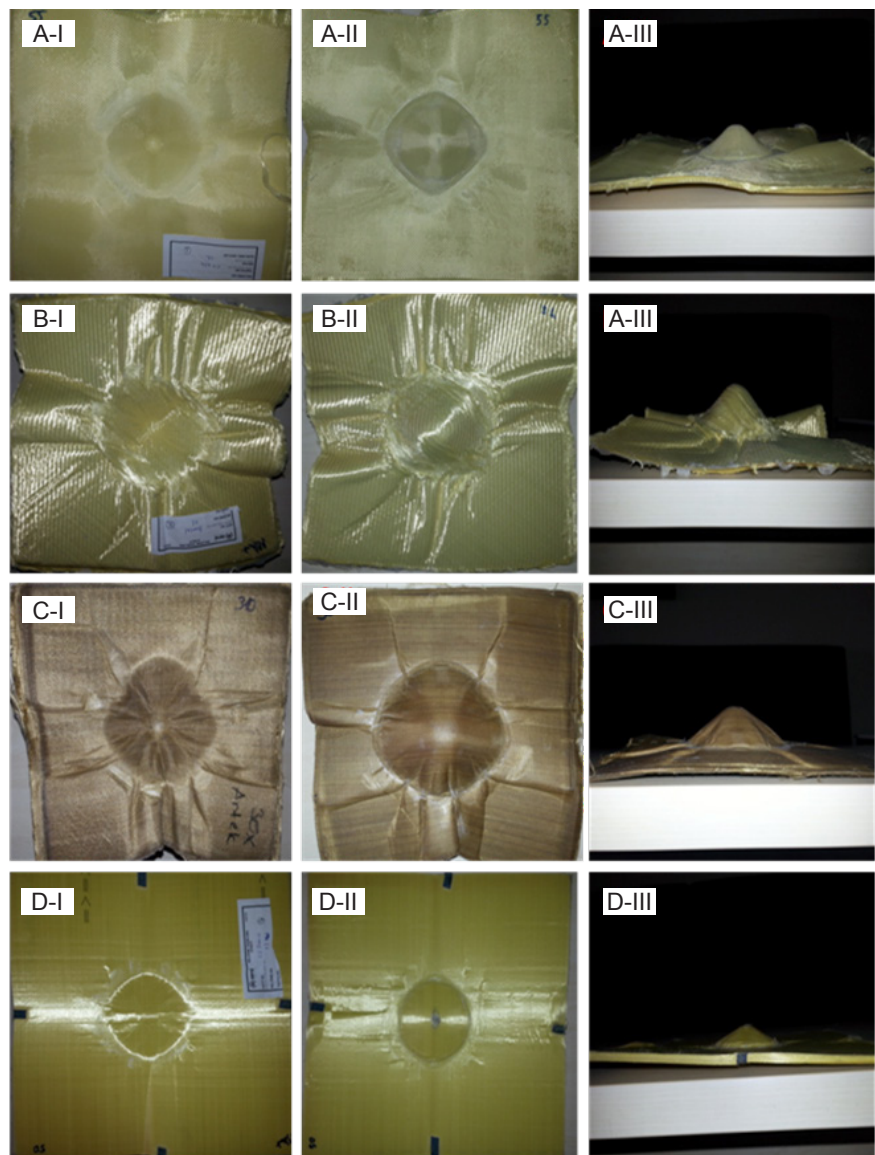


**Figure 4.a.** Images of damage occurring at impact locations on the top (I) and bottom surfaces (II) and cross-section (III) of composite samples for 1680-J impact energy (A, B, C and D, indicate the sample codes).

In terms of the maximum force, the 100% aramid samples were ranked in the following order: D, C, A, and B. The maximum force values of samples D and C were very high, and that of sample D was 30% more than that of sample A, 100% more than that of sample B, and 15% more than that of sample C. The fabric structure and fibre mechanical properties caused these differences. Although sample D was composed of woven fabric, the maximum force value was higher than that of the others due to the low crimp on the yarn caused by the thin yarn. It is known that lower crimp amounts result in higher mechanical properties [16, 22, 23]. Although samples A and B were produced from the same yarn and the mass per unit area was approximately equal, the maximum force value of sample A was 30% higher than that of sample B.

There was no crimp on the yarn in sample B, and therefore its impact behaviour was expected to be better than that of sample A, similar to the other mechanical properties [16]. However, the results indicate that the maximum force value of sample B was lower than that of sample A, which was composed of woven fabric. This paradox could be explained by deformation of the filament by the needle resulting from friction between the needle and yarn during bi-axial fabric manufacturing. Other researchers have also reported this situation [24 - 26].

The main differences between samples C and A were the linear density and threads per unit length of the weft and warp yarns. Both of these parameters determine the fibre volume fraction of composite samples. This factor greatly affects

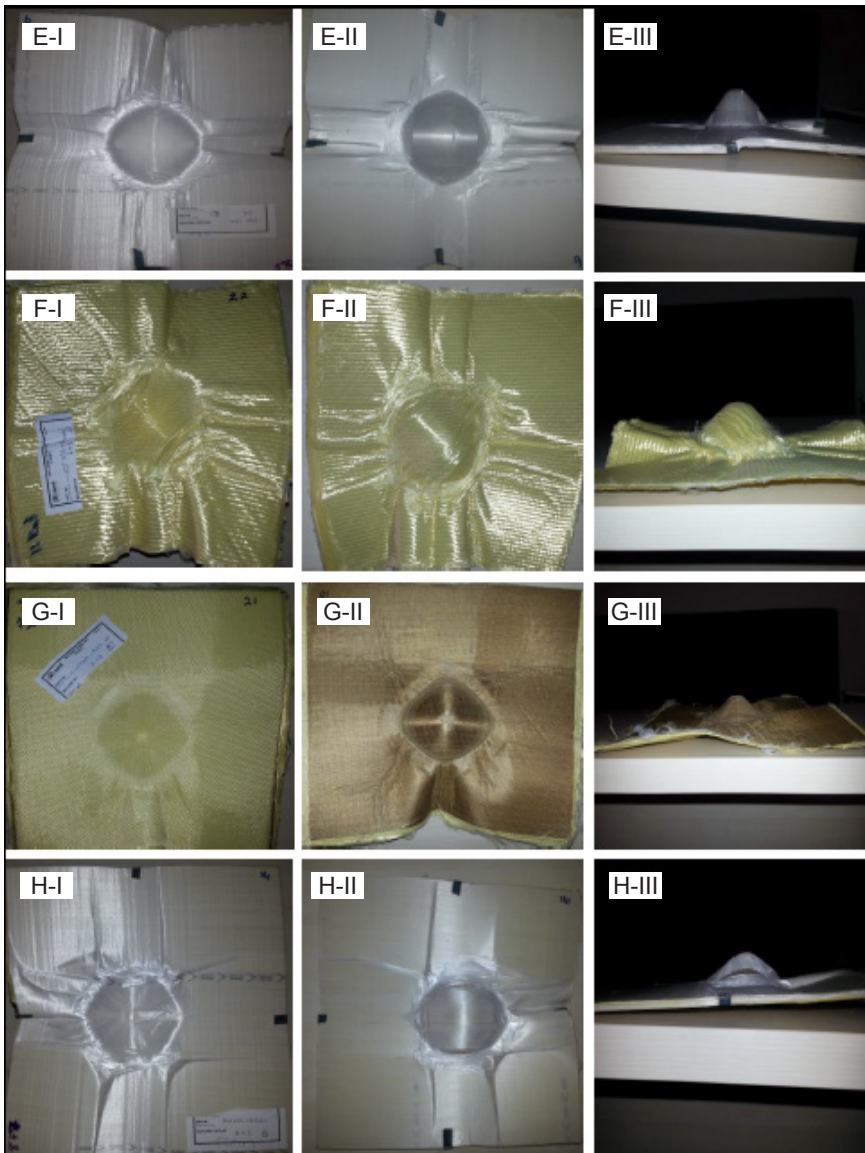


**Figure 4.b.** Images of damage occurring at impact locations on the top (I) and bottom surfaces (II) and cross-section (III) of composite samples for 1680 J impact energy (E, F, G and H indicate the sample codes).

the general mechanical and also impact behaviour of the composite structure, as observed in **Figure 2**.

The main differences between samples D and B were the cross-plyed degree and construction. Sample D was produced using the lay-out method, while B was made using a biaxial warp knitting machine. An adhesive film keeps the cross-plyed yarn system together in sample D, while the knitting yarns bond two layers of aramid yarn with loops in sample B. Therefore the layers in D 's structure are denser in contact than for sample B. The position of yarn in sample D is not changed due to the adhesive film, whereas the position of yarn may be altered in sample B when a force is encountered. These two parameters also affect the composite impact properties.

The maximum force and energy absorbed decreased and the time for maximum energy, displacement at the maximum energy, energy at the maximum force, displacement at the maximum force and time for the maximum force increased when using 45/45 cross-plyed aramid yarns, which were converted into fabric using loops instead of 0/90 cross-plyed aramid yarns. This result demonstrates that the flexibility of 45/45 cross-plyed fabric B was greater than that of the 0/90 cross-plyed structure. The impact strength of the 0/90 cross-plyed structure was greater than that of 45/45 cross-plyed fabric B. The following reasons may explain these findings:

a) These findings may occur because of damage to the yarn by needles taking place during the knitting process.

b) These findings may occur because the yarns in structure B's layers behave separately due to the loose loops; however, the yarns in sample D may be not separated because of the adhesive film between yarn layers.

This fact may occur because structure B was more flexible than structure D.

The main difference between samples D and E was the material type. The mass per unit area was nearly similar, and the effect of the mass per unit area negligible. Therefore the amount of resin between filaments can be considered to be the same. The material type also affects the impact properties of composite materials. Using UHMWPE filaments instead of aramid yarn in the composite as a reinforcement increases the time for maximum energy, displacement at maximum energy, energy and displacement at the maximum force, and the time for maximum force but decreases the maximum force and maximum energy absorbed. These effects arise from the filamentation and delamination of the UHMWPE sheets. In contrast to sample D, which was not filamented and delaminated, sample E was delaminated and filamented during impact testing. Therefore, the maximum force and maximum energy absorbed of sample D were higher than those of sample E. The displacement and time for the maximum force and energy absorbed of sample D were lower than those for sample E.

Although the maximum forces of the UHMWPE composite samples were lower than those of the aramid composite ones, the weights of the UHMWPE composite samples were also lower than those of the aramid ones. This advantage suggests the use of UHMWPE composites instead of aramid composites. Sample E, which was a UHMWPE composite, and sample D, which was an aramid composite, had the same construction. However, the maximum force of sample E was 67% less than that of sample D. As regards the weight of the samples, to obtain the force/weight per unit area ratio (specific force), the difference between sample E and sample D decreases to 32%. Therefore UHMWPE composites could be used with aramid composites or alone if weight optimisation is required. Aramid composites D and C yielded minimum displacement values. Less displacement offers more advantages for composites, where that of sample D is superior compared with that of the other seven samples. The displacements of all of the

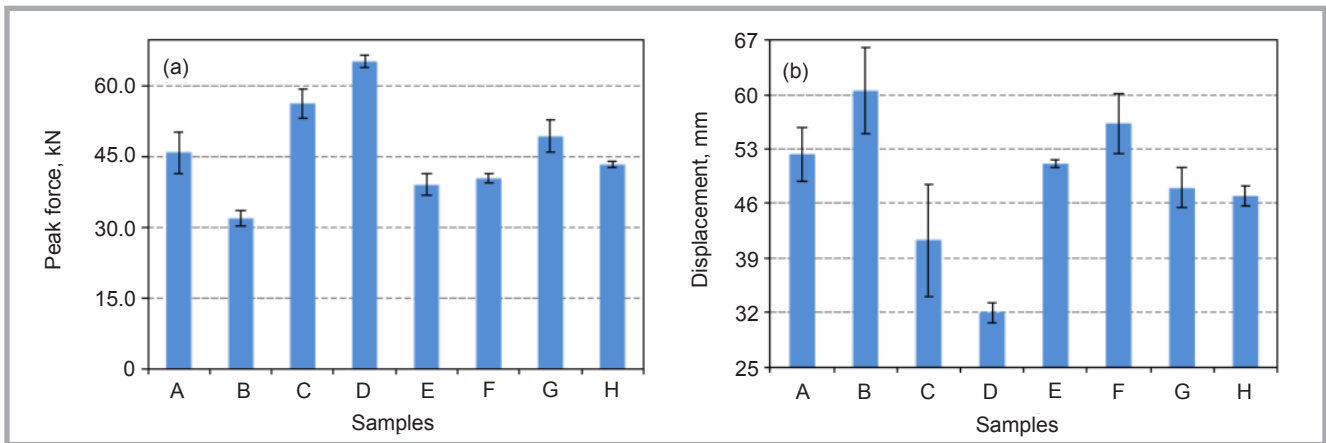


**Figure 5.** Comparison of peak force (a) and displacement of various samples.

samples are presented in **Figure 5.b**. The displacement of sample D was 63% lower than for sample A, 89% lower than for sample B, 29% lower than for sample C, 59% lower than for sample E, 75% lower than for sample F, 50% lower than for sample G and 46% lower than for sample H. Sample B exhibits the maximum displacement value, therefore exhibiting the poorest properties with respect to the displacement parameter. This situation was also noted in the maximum force section and was thought to be related to filament deformation.

With respect to the displacement parameter, sample E was better than samples A and B but worse than samples D and C. The displacement of sample E was 59% and 24% more than that of samples D and C, respectively. Although UHMWPE composites, such as sample E, have disadvantages, these composites can be preferred and used in the form of hybrids or alone because of weight advantages.

The hybridisation of different reinforcements in composite material yield new materials which are expected to exhibit different mechanical properties. The new material can retain the advantages of its constituents or produce undesirable mechanical properties. Hybridisation can also be used for weight optimisation of the composite. In this study, the aramid/UHMWPE hybrid structure was used for weight optimisation and the aramid/aramid hybrid structure applied for optimisation of the mechanical properties.

Sample F, which has an A/B structure, is an example of an aramid/aramid hybrid, the structure of which is composed of the same filament but with a different cross-ply condition and fabric structure. The hybrid structure has a 0/90/45/-45 cross-ply situation resulting from using

sample A, which is 0/90 cross-ply, and sample B, which is 45/-45 cross-ply, together. The 0/90 cross-ply section was woven fabric, and the 45/-45 cross-ply part - bi-axial knitting fabric. The aim of producing this type of hybrid was to investigate the effect of filament orientation and fabric structure on the impact properties of the composite. The maximum force of sample A was 30% more than that of sample B. The maximum force value of sample F, which was a hybrid of samples A and B, was 26% greater than that of sample B, as observed in **Figure 2**. The displacement property of the hybrid was also different from each component. The displacement value of sample B was 15% higher than that of sample A. The hybrid structure of these two reinforcements produced 8% better displacement than for sample B (**Figure 3**). Hybrid structure F is located between samples A and B with respect to both the maximum force and displacement properties.

Artec fibre is known as a high modulus fibre, and its mechanical properties are very good. Therefore this fibre is a solution in terms of the cost effective factor in ballistic composite manufacturing. Artec is a woven fabric and could thus be hybridised properly with sample A, which is also a woven fabric. The maximum force of sample A was 22% lower than that of sample C. The maximum force of sample G, which was a hybrid of samples A and C, was 7% greater than that of sample A (**Figure 2**). The same condition was also observed in the case of displacement. The displacement value of sample G was 10% lower and better than that of sample A (**Figure 3**).

It is known that the most popular aim of hybridisation is weight optimisation. Both aramid and UHMWPE filaments

have high-energy absorption properties. Due to the low density properties of UHMWPE filaments, the use of this material as a reinforcement in composite production is a state-of-the-art approach when weight is important.

While the stiffness of the UD UHMWPE sample (E) is moderate, sample D, which is UD aramid, is highly rigid. The maximum force of the UD aramid composite was 40% greater than that of the UD UHMWPE composite. The maximum force of sample H, which was produced by the hybridisation of samples D and E of the same thickness, was 10% greater than that of sample E (**Figure 2**). The same improvement was also achieved in the displacement properties, as observed in **Figure 3**. The displacement of sample H was 14% better than that of sample E. Hybrid H exhibited less displacement than sample E.

The deformation shape can be observed in **Figure 4**. The deformation forms of all the composite materials are different from each other in terms of the depth and, shape of the deformation as well as the composite surface outside of the deforming area. Not all of the composite structure was punctured. Deformation occurred and only formed a pit via extension type deformation of the reinforcement surface.

The shape of the pit mouth was different for changing reinforcement conditions. The mouth of the pit was square-shaped if the reinforcement was woven fabric due to stress concentration occurring at the weft and warp yarn interlacing point [27]. Because of the lack of yarn interlacing points for the UD cross-ply reinforcement, the mouth of the pit was conical-shaped. The mouth of the pit of the biaxial reinforcement was elliptical due

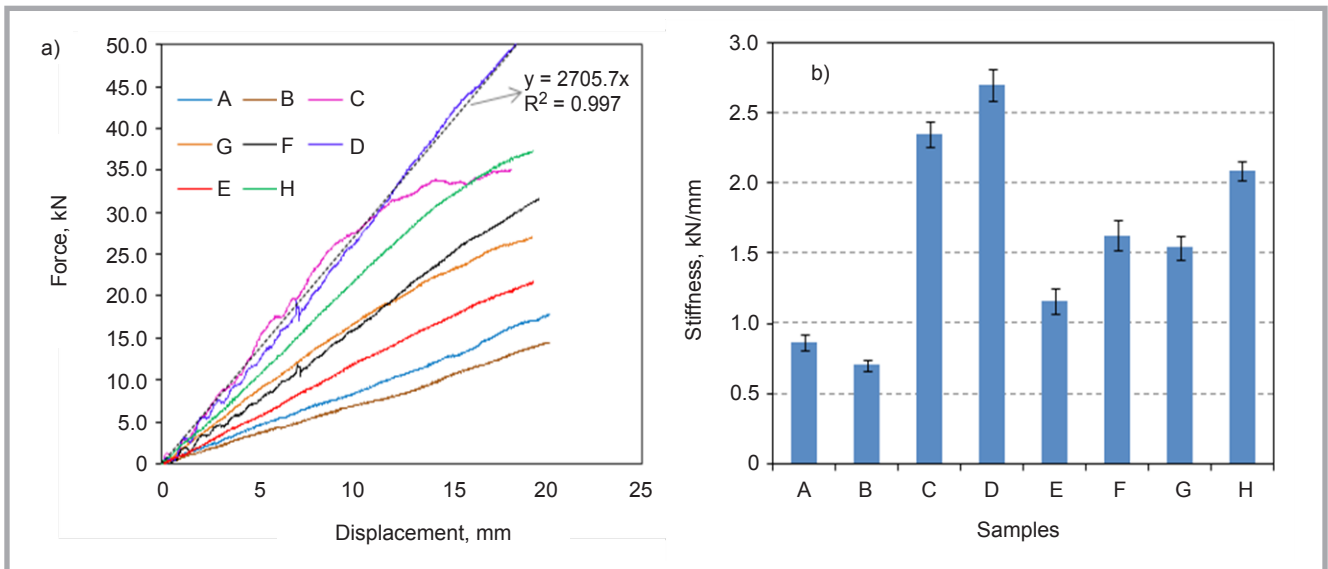


**Figure 6.** a) Initial section of load-displacement curves of various samples and slope of the load-displacement curve; b) comparison of bending stiffness values of various samples.

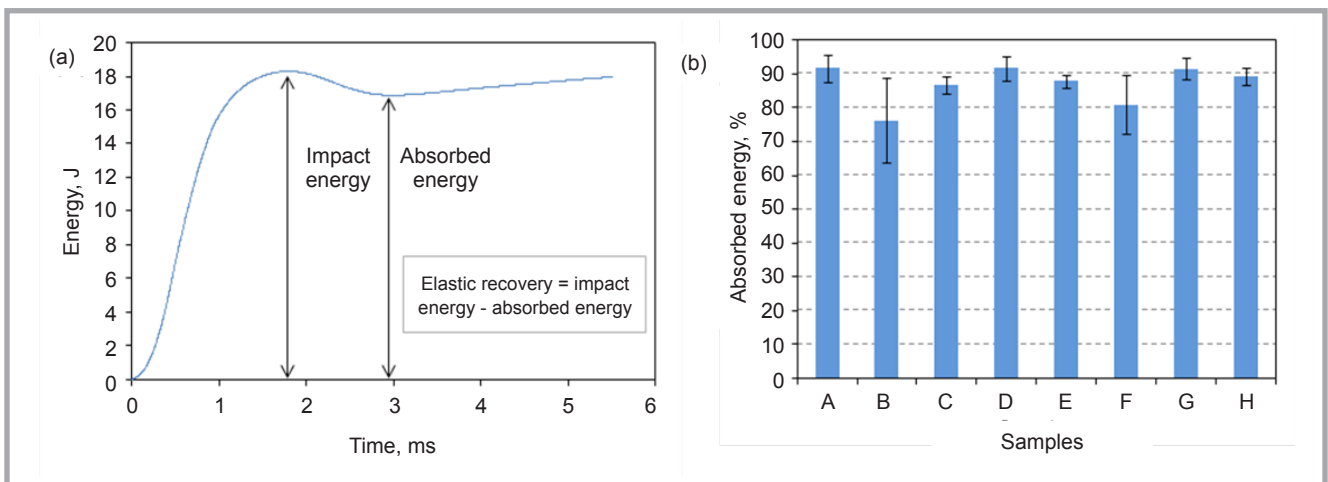


**Figure 7.** a) Typical energy – time curve and relationship between the elastic recovery energy, energy absorbed, and total impact energy. b) Percentage of energy absorbed by various samples.

to the 45/45 cross-piled aramid yarns. The hybrid structure of sample G, which was composed of two different woven reinforcements, exhibits the character of the reinforcement type with respect to the mouth of the pit being square-shaped. The mouth shape of the other hybrid structures, samples F and H, was conical, similar to the UD cross-plyed reinforcement.

In addition to pit formation due to the striker impact, the surfaces of all the composite materials was changed. Although slight deformation on composite A was observed, no damage occurred on the front and back surface of this sample. Filament breakage, filamentation and loop yarn breakage between the clamping point and peak of the tip of both sides of composite B were observed with moderate shape deformation. Surface damage

on the clamping point of both sides of composite C was also observed in addition to slight surface-shape deformation. Although slight surface damage occurred on the clamping point of the front side of composite D, filament breakage and serious surface damage occurred on the reverse side near the pit area. Along the surface and on the reverse side, delamination was also observed. Filament breakage and filamentation between the clamping point and peak of the tip of both sides of composite E were observed, with moderate shape deformation and delamination along the surface. The damage profile of composite F was a mixture of the damage observed for composites A and B. The front surface, which was composed of a reinforcement similar to that in composite B, exhibited B-type deformation, and the back surface, which was composed of a reinforcement similar

to that in composite A, showed A-type deformation.

The damage profile of composite G was similar to that of composite A. The damage profile of composite H was similar to that of samples D and E; differences between samples H, D and E were only in the tip depths, with the tip depth being higher on sample E than on sample H, and that on sample H higher than that of sample D.

### Bending stiffness of samples

The effect of the reinforcement properties and hybridisation on the impact properties of the composites can be examined using the maximum force and displacement amount data. In addition to this type of evaluation, determining the bending stiffness is very useful. David-West et al. [28] determined the bending

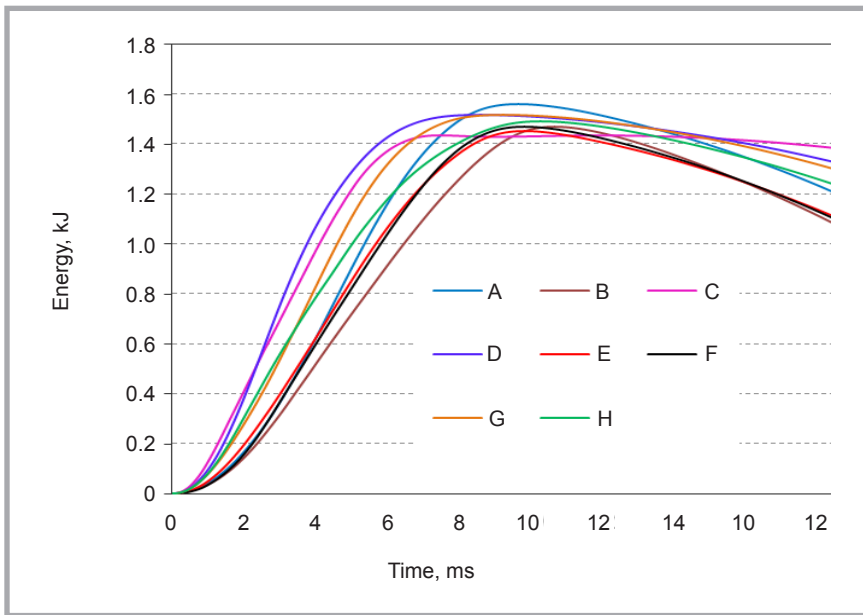


**Figure 8.** Typical impact energy–time curves and comparisons of all samples (A, B, C, D, E, F, G and H indicate the sample codes).

stiffness term as the slope of the curve in the elastic region on the load–displacement curve.

The impact bending stiffness is known as an important property in assessing the damage resistance of a composite, in particular delamination. This property changes with the configuration of the composite.

The slope of the ascending section of the load–displacement curve is the bending stiffness due to its representation of the stiffness of the plate under impact-induced bending at the beginning of the impact regime (**Figure 6.a**). The gradient of the best-fit line gives the stiffness values, with an  $R^2$  value of approximately 0.99. The force–displacement plots for the samples are quite different from each other, indicating different bending stiffnesses. A comparison of these values is presented in **Table 4**.

The elasticity of the fibre is higher than that of the matrix in textile-reinforced composite materials. Therefore the time required to reach the maximum force increases with the decreasing fibre volume fraction of the composite [29]. According to this information, D is the most rigid and B the most flexible materials among the 8 samples. The time for maximum energy is related to the end of deformation of the samples. Sample B absorbed energy in more time than the others, which also indicates that it is the most flexible material.

For sample D, the tangent stiffness increases until the peak load is reached. In addition, the unloading time was relatively shorter compared with the loading period. In general, the collision between the impactor and sample is inelastic, and hence the interaction forces between colliding bodies are non-conservative, with some energy being lost during loading and unloading. It is expected that the amount of energy absorbed could serve as an indicator of the extent of damage in the low-velocity impact.

Samples D and C exhibited the highest bending stiffness values, which was also supported by the deflection amount of the sample undersides (**Figure 4**). The displacement amount was observed to decrease with increasing bending stiffness. The bending stiffness values for all of the samples can be observed in **Figure 6.b**. The damage character of those with the highest bending stiffnesses (samples D and C) was different from the others.

### Energy absorption

The amount of energy absorbed ( $E_{abs}$ ) by the samples in the impact tests was calculated using the following formula:

$$E_{abs} = \frac{m}{2}(v_0^2 - v_{end}^2) \quad (2)$$

where,  $m$  is the total mass of the impacting assembly. The initial impact velocity  $v_0$  is obtained from the slope of the measured displacement–time curves just

before the impact. Here,  $v_{end}$  is the end velocity at the moment of loss of contact between the test specimen and the impact head, which is calculated from the displacement–time curve.

**Figure 7.a** shows the relationships between the total impact energy, energy absorbed, and the elastic recovery energy. The energy absorbed during impact is given in **Table 4**. **Figure 7.b** compares the percentage of energy absorbed for all the samples.

The best result was acquired from samples A, D and G with respect to the energy absorption behaviour, where there was no meaningful difference between the absorption capacities of these three. The energy absorption capacities of samples B and F were the worst, with sample B exhibiting the lowest energy absorption value. These conditions demonstrate that the bi-axial composite is not good in terms of impact behaviour, in contrast to expectations.

The energy absorption of some of the composites could be improved by using a hybrid structure. **Figure 8** presents the energy–time curves of all the composites. Energy absorption capacities of the hybrid samples are also given in **Figure 8** compared with 100% aramid and 100% UHMWPE samples. According to these results, the best hybridisation was obtained for sample G in relation to energy absorption. The energy absorption capacity of sample G was better than for both samples (A and C) forming sample G. In particular, the energy absorption character of sample G was 56% higher than that of sample C.

The energy absorption capacity of hybrid H, which was produced from samples D and E, was also good. In addition to the high energy absorption properties, the weight of sample H decreased when using the UHMWPE reinforcement. Therefore sample H may be useful when weight is an important parameter.

These results have demonstrated that the energy absorption features of laminate composites are considerably low compared with those of sandwich composites [29], which can be explained by the fact that in laminate composites propagation of the impact energy to the sample surface is very high.

The interlacing of energy absorbed and displacement curves occurred where the force was nearly at a maximum value for all of the samples. After the maximum force, unlike the energy absorbed, for which the level of increase did not change, the level of increase of the displacement decreased. The energy absorbed decreased after the maximum point of energy, except for sample C. Therefore another interlacing occurred between the energy absorbed and displacement curves at 12 - 14 ms. There was no decrease in the energy absorbed for sample C.

The amount of energy absorbed at the maximum force changed depending on the sample. Sample B absorbed the most energy and sample D the least at the maximum force value.

## Conclusions

In this study, the impact behaviour of 100% aramid, 100% UHMWPE, aramid-aramid hybrid and aramid-UHMWPE hybrid composites was investigated experimentally, the results of which are as follows:

- The 100% UD aramid composite plates (Sample D) have the highest peak load and lowest displacement. UD aramid was better than the other aramid-based composite with respect to both the maximum force and displacement.
- The maximum force and displacement value of the 100% Artec aramid composite were better than those of all of the other aramid-based composites.
- The worst value was acquired for the 100% aramid non-crimped bi-axial fabric reinforced composite with respect to all parameters, such as energy absorption, maximum force and displacement amount.
- UD aramid and Artec fabric yielded the best results with respect to the bending stiffness. The deflection amounts on the underside of UD aramid and Artec fabric were also the lowest.
- It was concluded that weight optimisation and improvement of the impact properties and energy absorption could be achieved by hybridisation of the reinforcement type.
- The maximum energy was absorbed by sample A and the minimum by sample C among the eight samples.

## References

1. Abrate S. Impact on laminated composite materials. *ASME Appl. Mech. Rev.* 1991; 44(2): 155-90.
2. Abrate S. Impact on laminated composites: recent advances. *ASME Appl. Mech. Rev.* 1994; 47(11): 517-44.
3. Wu E, Liao J. Impact of unstitched and stitched laminates by line loading. *J. Composite Materials* 1994; 28(17): 1640-58.
4. Wu E, Wang J. Behavior of stitched laminates under in-plane tensile and transverse impact loading. *J. Composite Materials* 1995; 29(11): 2254-79.
5. Wu E, Chang LC. Loading rate effect on woven glass laminated plates by penetration force. *J. Composite Materials* 1998; 32(8): 702-721.
6. Liu D. Impact-induced delamination – a view of bending stiffness mismatching. *J. Composite Materials* 1988; 22: 674-692.
7. Wu E, Shyu K. Response of composite laminates to contact loads and relationship to low-velocity impact. *J. Composite Materials* 1993; 27: 1443-64.
8. Evans RE, Masters JE. A new generation of epoxy composites for primary structural applications: materials and mechanics. ASTM 1985 STP 876 413-436.
9. Masters JE. Correlation of impact and delamination resistance in interleaved laminates. In: *6th ICCM/2th ICCM*, London, 3, 1987.
10. Mouritz AP, Leong KH, Herszberg I. A review of the effect of stitching on in-plane mechanical properties of fiber reinforced polymer composites. *Composites* 1997; 28A: 979-991.
11. Freitas G, Magee C, Dardzinski P, Fusco T. Fiber insertion process for improved damage tolerance in aircraft laminates. *Journal of Advanced Materials* 1994; 36.
12. Cantwell WJ, Morton J. The impact resistance of composite materials – a review. *Composites* 1991; 22(5): 347-62.
13. Virostek SP, Dual J, Goldsmith W. Direct force measurement in normal and oblique impact of plates by projectiles. *Int. J. Impact Eng.* 1987; 6: 247-69.
14. Delfosse D, Pageau G, Bennett R, Poursartip A. Instrumented impact testing at high velocities. *J. Composites Technol. Res.* 1993; 15(1): 38-45.
15. Zuoguang Z, Huancheng S. *Hybrid fiber composites* (in Chinese). Beijing University of Aeronautics and Astronautics Press, 1988.
16. Karahan M. Comparison of Ballistic Performance and Energy Absorption Capabilities of Woven and Unidirectional Aramid Fabrics. *Textile Research Journal* 2008; 78(8):718-730.
17. Karahan M, Kus A, Eren R. An Investigation into Ballistic Performance and Energy Absorption Capabilities of Woven Aramid Fabrics. *International Journal of Impact Engineering* 2008; 35, 6: 499–510.
18. Karahan M, Karahan N. Effect of Weaving Structure and Hybridization on the Low-Velocity Impact Behavior of Woven Carbon-Epoxy Composites. *Fibres & Textiles in Eastern Europe* 2014; 22, 3(105): 19-25.
19. Charrier JM. *Polymeric Materials and Processing*. Ed. Hanser, New York, USA, p.63, 1990.
20. Yıldırım K, Özcagatay U, Kostem AM, Güçer S. Analytical method for determination PE types, 12. Tekstil Teknolojisinde ve Kimyasındaki Son Gelişmeler Sempozyumu, TMMOB-Chambers of chemical Engineers, Bursa, 6-8 May, 2009.
21. Aslan Z, Karakuzu R, Sayman O. Dynamic Characteristics Of Laminated Woven E-Glass-Epoxy Composite Plates Subjected To Low Velocity Heavy Mass Impact. *J. Compos. Mater.* 2002; 36 (21): 2421-2442.
22. Karahan M, Ulcay Y, Eren R, Karahan N, Kaynak G. Investigation into the Tensile Properties of Stitched and Unstitched Woven Aramid/Vinyl Ester Composites. *Textile Research Journal* 2010; 80, 10: 880–891.
23. Karahan M, Ulcay Y, Karahan N, Kus A. Influence of Stitching Parameters on Tensile Strength of Aramid/Vinyl Ester Composites. *Materials Science (Medziagotyra)* 2013; 19(1): 67-72.
24. Mittal RK, Jafri MS. Influence of fibre content and impactor parameters on transverse impact response of uniaxially reinforced composite plates. *Composites* 1995; 26 (12): 877.
25. Flanagan MP, Zikry MA, Wall JW, El-Shiekh A. An Experimental Investigation of High Velocity Impact and Penetration Failure Modes in Textile Composites. *Journal of Composite Materials* 1999; 33(12): 1080-1103.
26. Padaki NV, Alagirusamy R, Deopura BL, Sugun BS, Fanguero R. Low velocity impact behaviour of textile reinforced composites. *Indian Journal of Fiber&Textile Research* 2008; 33: 189-202.
27. Karahan M, Karahan N. Influence of weaving structure and hybridization on the tensile properties of woven carbon-epoxy composites. *Journal of Reinforced Plastics and Composites* 2014; 33(2): 212–222.
28. David-West OS, Nash DH, Banks WM. An experimental study of the damage accumulation in balanced CFRP laminates due to repeated impact. *Composite Structures* 2008; 83: 247-258.
29. Karahan M, Gul H, Ivens J, Karahan N. Low velocity impact characteristic of 3D integrated core sandwich composites. *Textile Research Journal* 2012; 82(9): 845–862.

Received 04.08.2014 Reviewed 09.10.2014

**European Polysaccharide  
Network of Excellence**



**Institute of Biopolymers  
and Chemical Fibres**



**American Chemical  
Society**



**EPNOE 2015  
4th EPNOE International Polysaccharide Conference**

**POLYSACCHARIDES AND POLYSACCHARIDE  
-BASED ADVANCED MATERIALS:  
FROM SCIENCE TO INDUSTRY**

**National Stadium in Warsaw, Poland  
19 - 22 October 2015**

**organized by  
the Institute of Biopolymers and Chemical Fibres (IBWCh), Łódź, Poland**

EPNOE International Polysaccharide Conferences are now key features of the calendar of European scientific events. The conference has been organized biannually since 2009.

The conference aim is to bring together students, scientists and specialists working in industry, universities and research institutes to exchange experiences, present research results, develop a platform for mutual scientific contacts and intensify academic/industry cooperation.

Since 2013, the EPNOE International Polysaccharide Conference has been promoted and organised jointly by the European Polysaccharide Network of Excellence (**EPNOE**) and the Cellulose and Renewable Materials division of the American Chemical Society (**ACS**).

**On behalf of EPNOE and ACS, we have the pleasure to invite you to participate in the 4th Conference EPNOE 2015 "Polysaccharides and Polysaccharide - based advanced materials: From Science to Industry"**

**Scope of the conference:**

- Polysaccharide biosynthesis: structural and chemical aspects
- Polysaccharide dis-assembling, isolation and extraction
- Physical, structural, surface and chemical characterisation of polysaccharides
- Chemical and enzymatic degradation, functionalisation and modification of polysaccharides
- Nanopolysaccharide production, characterisation and uses, including nanocellulose and MFC
- Polysaccharides in food and feed
- Polysaccharides in health care, personal care, and cosmetics
- Materials for green engineering and building construction
- Biorefinery (pulp & paper, use of co-products and wastes)
- Bioplastics and fiber-reinforced composites
- Bio-resource and bio-product engineering
- Bio-based economy
- Bio-based textiles: eco-friendly design and technology

**Contact:**

***<http://epnoe2015.ibwch.lodz.pl>, e-mail: [epnoe2015@ibwch.lodz.pl](mailto:epnoe2015@ibwch.lodz.pl),  
phone: +48 42 638 03 02***